Electronic Supplementary Material (ESI) for Nanoscale.

Electronic Supplementally Information (ESI)

Lateral-Size Control of Exfoliated Transition-Metal-Oxide 2D Materials by Machine Learning on Small Data

Ryosuke Mizuguchi,[1] Yasuhiko Igarashi,[2,3] Hiroaki Imai,[1] Yuya Oaki*[1,3]

[1]Department of Applied Chemistry, Faculty of Science and Technology, Keio University, 3-14-1 Hiyoshi, Kohoku-ku, Yokohama 223-8522, Japan

[2]Faculty of Engineering, Information and Systems, University of Tsukuba, 1-1-1 Tennodai, Tsukuba 305-8573, Japan

[3]JST, PRESTO, 4-1-8 Honcho, Kawaguchi, Saitama 332-0012, Japan

E-mail: oakiyuya@applc.keio.ac.jp

Contents

Experimental methods

Syntheses of the precursor layered composites. Syntheses of the layered composites were referred to our previous works for titanate,[44] manganate,[44] tungstate,[44] and $Co(OH)_2$.[42,44] The pristine layered niobate and tantalate were synthesized by the methods according to the literatures.[59–62] Protonated layered titanate (H-TiO_2, $H_{0.7}Ti_{1.825}\square_{0.175}O_4\cdot yH_2O$ (□: vacancy)) was synthesized by the ion-exchange reaction of layered cesium titanate.[12,44,R1] Sodium manganate (Na-MnO_2, $Na_xMn_{2-x}O_2\cdot yH_2O$) was synthesized by aqueous-solution method at room temperature.[44,R2] Protonated layered tungstate (H-WO_3, $HCs_3W_{11}O_{35}\cdot yH_2O$) was synthesized by the ion-exchange reaction of layered cesium tungstate.[29,44,R3] Protonated layered niobate (H-Nb_2O_5, $H_{3.2}K_{0.8}Nb_6O_{17}\cdot yH_2O$) was synthesized by the ion-exchange reaction of layered potassium niobate.[59,60] Protonated layered tantalate (H-BST, $H_{1.8}Bi_{0.2}Sr_{0.8}Ta_2O_7\cdot yH_2O$) was synthesized by the ion-exchange reaction of layered bismuth strontium tantalate.[61,62] According to the size prediction in Table S3, the guest organic molecules were intercalated by the ion-exchange reaction of the protonated layered compounds, such as H-TiO_2, H-WO_3, H-Nb_2O_5, and H-BST, through the acid-base reaction.

The following guest amines were intercalated in the in the layered titanate: hexylamine (C_6-NH_2, TCI, 99.0 %), tetradecylamine (C_{14}-NH_2, TCI, 96.0 %), stearylamine (C_{18}-NH_2, TCI, 85.0 %), 4-methoxybenzylamine (OMe-BA, TCI, 97.0 %), 4-aminobenzylamine (NH_2-BA, TCI, 98.0 %), 4-(aminomethyl)phenol (OH-BA, TCI, 98.0 %), 4-methylbenzylamine (CH_3-BA, TCI, 98.0 %), benzylamine (H-BA, TCI, 99.0 %), 4-fluorobenzylamine (F-BA, TCI, 98.0 %), DL-1-(1-naphthyl)ethylamine (NEA, TCI, 98.0 %), 1-(3-aminopropyl)imidazole (API, TCI, 97.0 %), 3-thiophenemethylamine (Tp-MA, TCI, 97.0 %), and 3-butoxypropylamine (BPA, TCI, 98.0 %). These amines (0.823 mmol) were dissolved in purified water (50 cm^3). Then, 0.2 g of H-TiO_2 was added in the aqueous solution and then maintained for 10 days at room temperature under stirring. The molar ratio of the interlayer proton to the amine was adjusted to 1.0. The precipitates were centrifuged and washed by ethanol and tetrahydrofuran (THF). The resultant powder was dried at room temperature.

The following guest amines were intercalated in the in the layered manganate: C_6-NH_2, C_{14}-NH_2, NEA, API, 4-vinylbenzylamine (Vinyl-BA, TCI, 92.0 %), 4-(aminomethyl)benzonitrile hydrochloride (CN-BA, TCI, 85.0 %), and 2-(2-aminoethyl)pyridine (PEA, TCI, 98.0 %). Aqueous solution containing 0.1 mol dm^{-3} these amines was prepared using 60 cm^3 purified water. The pH of the solution was adjusted to 7.00 using hydrochloric acid (HCl). The precursor Na-MnO_2 was prepared in 1 dm^3 scale.[44,R2] All the resultant Na-MnO_2 powder in the wet state was dispersed in the aqueous solution containing the amine. After pH of the solution was adjusted to 7.00 again, the solution was maintained for 24 h at room temperature under stirring. The resultant precipitates were centrifuged and washed by the mixture of ethanol and purified water.

The following guest amines were intercalated in the in the layered tungstate: C_6-NH_2, C_{14}-

NH_2, CH_3-BA, H-BA, Vinyl-BA, BPA, PEA, and 2-(2-aminoethyl)thiophene (Tp-EA, TCI, 97.0 %). These amines (5 mmol) were dissolved in purified water (80 cm^3). Then, 0.3 g of H-WO_3 was dispersed in the aqueous solution for 10 days at room temperature under stirring. The molar ratio of the interlayer proton to the amine was adjusted to 50. The resultant precipitates were centrifuged and washed by ethanol and THF. The powder was dried at room temperature.

The following guest amines were intercalated in the in the layered niobate: C_6-NH_2, CH_3-BA, API, PEA, Tp-EA, diaminomaleonitrile (DAMN, TCI, 96.0 %), and diethanolamine (DEA, TCI, 99.0 %). These amines (2 mmol) were dissolved in purified water (100 cm^3). Then, 0.5 g of H-Nb_2O_5 was dispersed in the aqueous solution for 10 days at room temperature under stirring. The molar ratio of the interlayer proton to the amine was adjusted to 1. The resultant precipitates were centrifuged and washed by ethanol and THF. The powder was dried at room temperature.

The following guest amines were intercalated in the in the layered tantalate: C_6-NH_2, C_{14}-NH_2, CH_3-BA, F-BA, Vinyl-BA, and PEA, and DAMN. These amines (0.6 mmol) were dissolved in purified water (30 cm^3). Then, 0.2 g of H-BST was added in the aqueous solution for 10 days at room temperature under stirring. The molar ratio of the interlayer proton to the amine was adjusted to 1. The resultant precipitates were centrifuged and washed by ethanol and THF. The powder was dried at room temperature.

The following guest anions were directly introduced in the anionic interlayer space of alpha-type cobalt hydroxide (α-$Co(OH)_2$):[42,44,R4] heptanoic acid (C_6-COOH, TCI, 98.0 %), sodium dodecyl sulfate (TDS, TCI, 97.0 %), *p*-tolylacetic acid (CH_3-PA, TCI, 98.0 %), sodium anthraquinone-2-sulfonate monohydrate (AQ-SA, TCI, 98.0 %), and 4-butoxyphenylacetic acid (BuO-PA, TCI, 98.0 %). An aqueous solution containing 0.238 g cobalt chloride hexahydrate ($CoCl_2 \cdot 6H_2O$, Wako, 99.0 %) and 2.0 mmol these amines was prepared using 30 cm^3 purified water. This sample bottle and another sample bottle containing 7.5 mol dm^{-3} ammonia were separately set in a larger vessel. Diffusion of ammonia vapor yields to form the precipitate in the sample bottle containing cobalt ions.[42,44,R4] After the sealing, the sample was maintained at room temperature for 2 days without stirring. The resultant precipitates were centrifuged and washed with purified water, ethanol and THF.

Characterization of the precursor layered composites. The interlayer distance of the layered composites was analyzed by powder X-ray diffraction (XRD, Bruker D8 Advance) with Cu-Kα radiation. The organic contents in the layered composites were measured by thermogravimetry (TG) analysis (Seiko TG-DTA 7000 and Shimadzu DTG-60) in air atmosphere. The particle size of the layered composites was measured by the images of field-emission scanning electron microscopy (FESEM, Hitachi S-4700 and JEOL JSM-7600F) operated at 5.0 kV. The composition of the layered composites was estimated from the TG curves according to the methods in our previous report (See Experimental Section in the Supporting Information).[44]

Exfoliation of the layered composites. The exfoliation experiments were only performed for the host-guest-medium combinations in Table S3 in the Supplemental Information according to the prediction. The resultant layered composites (30 mg) were dispersed in 12 cm^3 of certain organic media for 5 days at 60 °C under stirring around 300 rpm. The following dispersion media were used for the exfoliation (Table S3): purified water, benzaldehyde (Kanto, 99.0 %), ethylbenzene (Wako, 96.0 %), THF (Kanto, 99.5 %), formamide (Kanto, 98.0 %), 1,3-dioxolane (TCI, 98.0 %), and diethylene glycol (DEG, Kanto, 98.0 %). The resultant dispersion liquid containing the nanosheets was filtered using filter with 2.0 um in the pore size for titanate and cotton for the other compounds to remove the unexfoliated and/or bulky aggregated particles. Then, the particle-size distribution was immediately measured using dynamic light scattering (DLS, Otsuka Electronics, ELSZ-2000ZS). The nanosheets were observed by transmission electron microscopy (TEM, FEI, Tecnai G2 and F20). The dispersion liquid was dropped on a collodion membrane for TEM observations.

Preparation of the dataset and its analysis. The dataset containing explanatory and objective variables was prepared for sparse modelling. The explanatory variables were collected from the literatures and calculation data. The explanatory variables (x_n: n = 5, 6, 11, 12, 16, 17 in Table 2) were calculated by Gaussian 16W by density functional theory (DFT) with B3LYP based on the 6–311G basis set. The explanatory variables (x_n: n = 7–9, 11–13, 18) were calculated by Hansen Solubility Parameters in Practice (HSPiP, version 5.0.03). The L and L_0 values were measured by DLS and SEM, respectively. The size reduction rate ($R_L = L\, L_0^{-1}$) for the titanate in the training dataset was estimated from the data in our previous work.[43] A multiple regression analysis with penalty by MCP was performed on the training dataset containing the R_L as objective variables (y) and explanatory variables (x_{1-18}) using a free software R. The predicted R_L values were calculated by (eq. 1) with conversion of x_n to the normalized frequency distribution such that the mean is 0 and standard deviation is 1.

Additional references

R1. T. Sasaki, Y. Komatsu and Y. Fujiki, *J. Chem. Soc. Chem. Commun.*, 1991, 817.
R2. Y. Oaki and H. Imai, *Angew. Chem. Int. Ed.*, 2007, **46**, 4951.
R3. K. Fukuda, K. Akatsuka, Y. Ebina, M. Osada, W. Sugimoto, M. Kimura and T. Sasaki, *Inorg. Chem.*, 2012, **51**, 1540.
R4. Y. Oaki, S. Kajiyama, T. Nishimura and T. Kato, *J. Mater. Chem.*, 2008, **18**, 4140.

Training dataset for construction of size-prediction model

Table S1. Dataset containing the measured R_L values for the 48 guest-medium combinations and their explanatory variables (x_n: n= 1–18).[43]

No.	Guest molecules	Dispersion media	x_1 / g mol^{-1}	x_2 / °C	x_3 / °C	x_4 / g cm^{-3}	x_5 / D	x_6 / 10^{-40} (Cm)^2 J^{-1}	x_7 / –	x_8 / –	x_9 / –	x_{10} / g mol^{-1}	x_{11} / 10^{-40} (Cm)^2 J^{-1}	x_{12} / D	x_{13} / -	x_{14} / -	x_{15} / -	x_{16} / 10^{-40} (Cm)^2 J^{-1}	x_{17} / D	x_{18} / –	R_L / –	Yield / %
1	C_{14}-NH_2	NMP	99.13	-24.4	202	1.03	4.301	10.2	18	12.3	7.2	213.4	2.8	1.24	16.1	2.3	4.1	17.8	3.06	11.14	0.271	13.64
2	C_{14}-NH_2	DMF	73.09	-60.43	153	0.94	4.375	7.23	17.4	13.7	11.3	213.4	2.8	1.24	16.1	2.3	4.1	20.7	3.14	13.73	0.273	22.55
3	C_{14}-NH_2	DMSO	78.13	18.54	189	1.1	5.159	7.93	18.4	16.4	10.2	213.4	2.8	1.24	16.1	2.3	4.1	20	3.92	16.04	0.241	4.52
4	NH_2-BA	Water	18.02	0	100	1	2.429	0.864	15.5	16	42.3	122.2	1.46	1.26	19.9	7	12.2	13.8	1.17	32.63	0.162	62.15
5	NH_2-BA	Acetonitrile	41.05	-43.83	81.6	0.78	3.927	3.89	15.3	18	6.1	122.2	1.46	1.26	19.9	7	12.2	10.7	2.67	15.58	0.302	10.82
6	NH_2-BA	NMP	99.13	-24.4	202	1.03	4.301	10.2	18	12.3	7.2	122.2	1.46	1.26	19.9	7	12.2	4.43	3.04	8.22	0.138	11.99
7	NH_2-BA	DMF	73.09	-60.43	153	0.94	4.375	7.23	17.4	13.7	11.3	122.2	1.46	1.26	19.9	7	12.2	7.4	3.12	8.41	0.15	52.70
8	NH_2-BA	DMSO	78.13	18.54	189	1.1	5.159	7.93	18.4	16.4	10.2	122.2	1.46	1.26	19.9	7	12.2	6.69	3.9	10.07	0.23	36.63
9	CH_3-BA	Water	18.02	0	100	1	2.429	0.864	15.5	16	42.3	121.2	1.5	1.17	18.8	4.8	6.6	14.1	1.26	37.99	0.516	10.03
10	CH_3-BA	Acetonitrile	41.05	-43.83	81.6	0.78	3.927	3.89	15.3	18	6.1	121.2	1.5	1.17	18.8	4.8	6.6	14.1	1.26	37.99	0.212	7.81
11	CH_3-BA	Methanol	32.04	-97.68	64.6	0.79	2.106	2.65	15.1	12.3	22.3	121.2	1.5	1.17	18.8	4.8	6.6	12.3	0.94	18.91	0.326	14.05
12	CH_3-BA	NMP	99.13	-24.4	202	1.03	4.301	10.2	18	12.3	7.2	121.2	1.5	1.17	18.8	4.8	6.6	4.81	3.13	7.69	0.216	7.32
13	CH_3-BA	DMSO	78.13	18.54	189	1.1	5.159	7.93	18.4	16.4	10.2	121.2	1.5	1.17	18.8	4.8	6.6	7.07	3.99	12.17	0.202	4.53
14	BA	Methanol	32.04	-97.68	64.6	0.79	2.106	2.65	15.1	12.3	22.3	107.2	1.28	1.49	18.8	4.6	7.1	10.1	0.62	18.58	0.212	21.50
15	BA	Ethanol	46.07	-114.49	78.3	0.78	1.942	4.56	15.8	8.8	19.4	107.2	1.28	1.49	18.8	4.6	7.1	8.23	0.45	14.32	0.453	6.39
16	BA	Acetone	58.05	-94.7	58.1	0.78	3.228	5.9	15.5	10.4	7	107.2	1.28	1.49	18.8	4.6	7.1	6.89	1.74	8.79	0.208	12.19
17	BA	NMP	99.13	-24.4	202	1.03	4.301	10.2	18	12.3	7.2	107.2	1.28	1.49	18.8	4.6	7.1	2.6	2.81	7.87	0.198	4.12
18	BA	DMSO	78.13	18.54	189	1.1	5.159	7.93	18.4	16.4	10.2	107.2	1.28	1.49	18.8	4.6	7.1	4.86	3.67	12.23	0.482	9.48
19	F-BA	Water	18.02	0	100	1	2.429	8.64	15.5	16	42.3	125.2	1.28	3.61	18.7	6.2	7.3	11.9	1.18	36.91	0.12	5.31
20	F-BA	Acetonitrile	41.05	-43.83	81.6	0.78	3.927	3.89	15.3	18	6.1	125.2	1.28	3.61	18.7	6.2	7.3	8.9	0.32	13.67	0.174	3.32
21	F-BA	Methanol	32.04	-97.68	64.6	0.79	2.106	2.65	15.1	12.3	22.3	125.2	1.28	3.61	18.7	6.2	7.3	10.1	1.5	17.72	0.174	8.41
22	F-BA	Ethanol	46.07	-114.49	78.3	0.78	1.942	4.56	15.8	8.8	19.4	125.2	1.28	3.61	18.7	6.2	7.3	8.23	1.67	13.67	0.3	6.21
23	F-BA	DMF	73.09	-60.43	153	0.94	4.375	7.23	17.4	13.7	11.3	125.2	1.28	3.61	18.7	6.2	7.3	5.56	0.77	8.89	0.168	21.77
24	F-BA	DMSO	78.13	18.54	189	1.1	5.159	7.93	18.4	16.4	10.2	125.2	1.28	3.61	18.7	6.2	7.3	5.56	0.77	8.89	0.244	2.00
25	OH-BA	Water	18.02	0	100	1	2.429	0.864	15.5	16	42.3	123.2	1.36	1.83	19.6	7.2	13.4	12.8	0.6	31.3	0.148	65.81
26	OH-BA	Methanol	32.04	-97.68	64.6	0.79	2.106	2.65	15.1	12.3	22.3	123.2	1.36	1.83	19.6	7.2	13.4	11	0.27	13.65	0.155	48.83
27	OH-BA	Ethanol	46.07	-114.49	78.3	0.78	1.942	4.56	15.8	8.8	19.4	123.2	1.36	1.83	19.6	7.2	13.4	9.08	0.11	9.81	0.198	45.39
28	OH-BA	Acetone	58.05	-94.7	58.1	0.78	3.228	5.9	15.5	10.4	7	123.2	1.36	1.83	19.6	7.2	13.4	7.74	1.39	10.88	0.345	7.22
29	OH-BA	THF	72.11	-108.39	66	0.89	2.264	7.51	16.8	5.7	8	123.2	1.36	1.83	19.6	7.2	13.4	6.13	0.43	7.92	0.492	4.55
30	OH-BA	NMP	99.13	-24.4	202	1.03	4.301	10.2	18	12.3	7.2	123.2	1.36	1.83	19.6	7.2	13.4	3.45	2.47	8.64	0.202	57.10
31	OH-BA	DMF	73.09	-60.43	153	0.94	4.375	7.23	17.4	13.7	11.3	123.2	1.36	1.83	19.6	7.2	13.4	6.42	2.54	8.13	0.369	67.08
32	OH-BA	DMSO	78.13	18.54	189	1.1	5.159	7.93	18.4	16.4	10.2	123.2	1.36	1.83	19.6	7.2	13.4	5.71	3.32	10.03	0.157	73.05
33	Tp-CH_2NH_2	Water	18.02	0	100	1	2.429	0.864	15.5	16	42.3	113.2	1.19	2.09	19.3	5.6	10.1	11.1	0.34	34.68	0.179	59.67
34	Tp-CH_2NH_2	Methanol	32.04	-97.68	64.6	0.79	2.106	2.65	15.1	12.3	22.3	113.2	1.19	2.09	19.3	5.6	10.1	9.29	0.01	16.26	0.248	21.15
35	Tp-CH_2NH_2	Ethanol	46.07	-114.49	78.3	0.78	1.942	4.56	15.8	8.8	19.4	113.2	1.19	2.09	19.3	5.6	10.1	7.38	0.15	12.07	0.576	7.22
36	Tp-CH_2NH_2	Acetone	58.05	-94.7	58.1	0.78	3.228	5.9	15.5	10.4	7	113.2	1.19	2.09	19.3	5.6	10.1	6.03	1.13	9.51	0.228	5.36
37	Tp-CH_2NH_2	NMP	99.13	-24.4	202	1.03	4.301	10.2	18	12.3	7.2	113.2	1.19	2.09	19.3	5.6	10.1	1.74	2.21	7.75	0.241	14.26
38	Tp-CH_2NH_2	DMF	73.09	-60.43	153	0.94	4.375	7.23	17.4	13.7	11.3	113.2	1.19	2.09	19.3	5.6	10.1	4.71	2.28	9.03	0.306	22.07
39	Tp-CH_2NH_2	DMSO	78.13	18.54	189	1.1	5.159	7.93	18.4	16.4	10.2	113.2	1.19	2.09	19.3	5.6	10.1	4	3.07	10.95	0.222	15.38
40	Naph-EtNH_2	Water	18.02	0	100	1	2.429	0.864	15.5	16	42.3	171.2	2.23	1.45	19.5	4	5.9	21.5	0.98	39.15	0.164	10.44
41	Naph-EtNH_2	Acetonitrile	41.05	-43.83	81.6	0.78	3.927	3.89	15.3	18	6.1	171.2	2.23	1.45	19.5	4	5.9	18.5	2.48	16.33	0.309	5.08
42	Naph-EtNH_2	Methanol	32.04	-97.68	64.6	0.79	2.106	2.65	15.1	12.3	22.3	171.2	2.23	1.45	19.5	4	5.9	19.7	0.66	20.38	0.214	62.11
43	Naph-EtNH_2	Ethanol	46.07	-114.49	78.3	0.78	1.942	4.56	15.8	8.8	19.4	171.2	2.23	1.45	19.5	4	5.9	17.8	0.49	16.13	0.401	32.00
44	Naph-EtNH_2	Acetone	58.05	-94.7	58.1	0.78	3.228	5.9	15.5	10.4	7	171.2	2.23	1.45	19.5	4	5.9	16.4	1.78	10.3	0.331	12.98
45	Naph-EtNH_2	Chloroform	119.38	-63.52	61.2	1.48	1.528	6.53	17.8	3.1	5.7	171.2	2.23	1.45	19.5	4	5.9	15.8	0.08	3.52	0.308	55.34
46	Naph-EtNH_2	NMP	99.13	-24.4	202	1.03	4.301	10.2	18	12.3	7.2	171.2	2.23	1.45	19.5	4	5.9	12.2	2.85	8.92	0.141	44.12
47	Naph-EtNH_2	DMF	73.09	-60.43	153	0.94	4.375	7.23	17.4	13.7	11.3	171.2	2.23	1.45	19.5	4	5.9	15.1	2.93	11.87	0.501	44.11
48	Naph-EtNH_2	DMSO	78.13	18.54	189	1.1	5.159	7.93	18.4	16.4	10.2	171.2	2.23	1.45	19.5	4	5.9	14.4	3.71	13.31	0.427	7.39

SEM images of the precursor layered composites

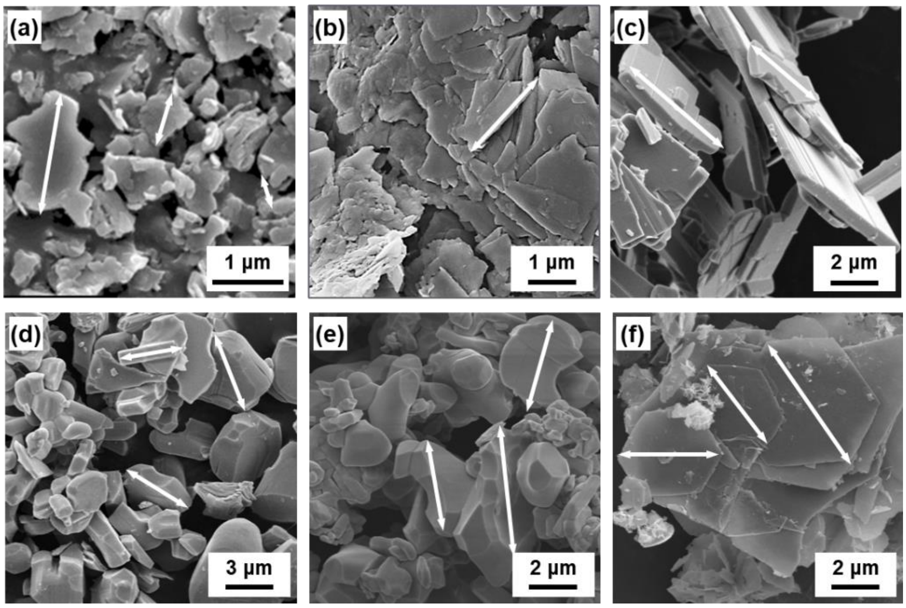

Fig. S1. SEM images of the precursor layered composites based on titanate (a), manganate (b), tungstate (c), niobate (d), tantalate (e), and $Co(OH)_2$ (f).

The average lateral size (L_{ave}) and its standard deviation (σ) were estimated from the sizes of the primary particles on the SEM images (Fig. S1). In the present work, the lateral size (L_0) was defined as $L_0 = L_{ave} + \sigma$. The L_0 values were calculated to be 1.52 µm for TiO_2, 3.66 µm for MnO_2, .4.78 µm for WO_3, 4.60 µm for Nb_2O_5, 2.75 µm for BST, and 3.72 µm for $Co(OH)_2$.

Unknown host-guest-medium combinations

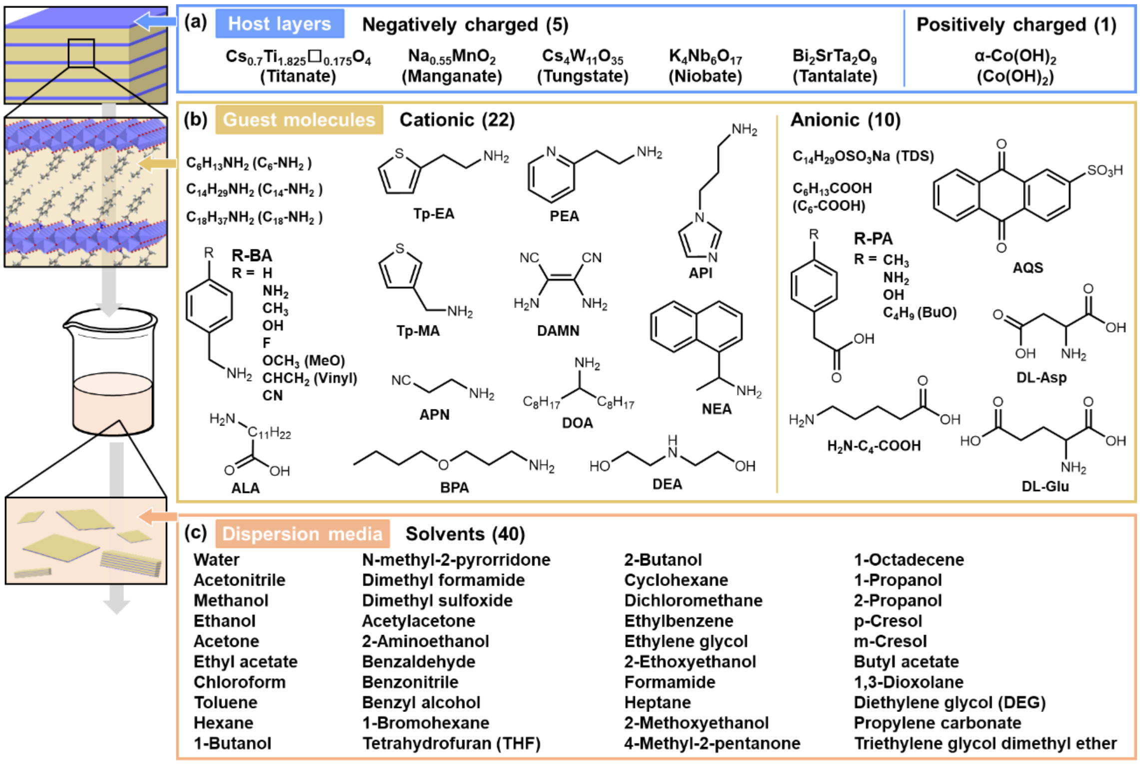

Fig. S2. Unknown host-guest-medium combinations for the test of prediction model. (a) Total 6 host layered compounds including the negatively (5) and positively (1) charged layered compounds. (b) Cationic (22) and anionic (10) guests for intercalation into the negatively and positively charged host layers, respectively. (c) Total 40 dispersion media for exfoliation of the layered composites.

Total 4400 host-guest-medium combinations were prepared for exfoliation of negatively charged host layers (5 × 22 × 40 combinations, the left side of Fig. S2). In addition, 400 guest-medium combinations were prepared for exfoliation of $Co(OH)_2$ (1 × 10 × 40 combinations, the right side of Fig. S2). Therefore, total 4800 unknown combinations were assumed to the exfoliation experiments.

These combinations to achieve the yield higher than 30 % were firstly extracted using the yield-prediction model in our previous work.[44] Then, the combinations to obtain large and small nanosheets were extracted using the size-prediction model (eq. 1) (Table S3). According to the two prediction models, the same predicted guest-medium combinations were prepared for negatively charged host layers. However, the combinations were different for each host layer (Table S3). When the target guest molecule was not experimentally intercalated, the next one was moved up in the rank. In this manner, the predicted conditions were prepared for the exfoliation experiments.

Summary of predicted and measured R_L for each host layer

Table S2. Unknown host-guest-medium combinations with the predicted larger and smaller R_L values and their measured ones.

Large-size nanosheets						Small-size nanosheets					
Titanate											
Rank	Guest molecules	Medium	Predicted R_L / -	Measured R_L / -	Yield / %	Rank	Guest molecules	Medium	Predicted R_L / -	Measured R_L / -	Yield / %
L-01	Vinyl-BA	THF	0.473	1.130	3.16	S-01	DAMN	Formamide	-0.567	0.179	3.67
L-02	H-BA	Benzaldehyde	0.469	0.182	6.47	S-02	API	DEG	-0.476	0.163	21.67
L-03	Vinyl-BA	Ethylbenzene	0.465	0.233	1.1	S-03	BPA	DEG	-0.460	0.310	25.64
L-04	NEA	1,3-Dioxolane	0.461	0.308	2.89	S-04	C_{18}-NH_2	DEG	-0.402	0.312	1.28
L-05	Tp-EA	THF	0.461	0.352	3.88	S-05	C_6-NH_2	DEG	-0.394	0.189	11.95
L-06	Tp-MA	Benzaldehyde	0.453	0.434	6.07	S-06	MeO-BA	DEG	-0.386	0.194	46.3
L-07	CH_3-BA	Benzaldehyde	0.451	0.334	19.9	S-07	F-BA	DEG	-0.382	0.117	4.51
L-08	DOA	THF	0.449	0.264	3.43	S-08	DOA	DEG	-0.368	0.200	3.6
L-09	H-BA	1,3-Dioxolane	0.445	0.354	5.79	S-09	Tp-EA	DEG	-0.337	0.118	20.1
L-10	NH_2-BA	1,3-Dioxolane	0.392	0.592	1.95	S-10	DEA	Formamide	-0.262	0.292	41.64
Average			0.452	0.418	5.46	Average			-0.403	0.207	18.04
Standard deviation			0.023	0.275	5.37	Standard deviation			0.083	0.073	16.15
Manganate											
Rank	Guest molecules	Medium	Predicted R_L / -	Measured R_L / -	Yield / %	Rank	Guest molecules	Medium	Predicted R_L / -	Measured R_L / -	Yield / %
L-01	NEA	Benzaldehyde	0.477	0.530	11.72	S-01	API	DEG	-0.476	0.034	0.587
L-02	Vinyl-BA	THF	0.473	0.500	54.35	S-02	PEA	DEG	-0.411	0.046	13.81
L-03	Vinyl-BA	Ethylbenzene	0.465	0.284	1.8	S-03	C_6-NH_2	DEG	-0.394	0.023	9.11
L-04	NEA	1,3-Dioxolane	0.461	0.817	42.47	S-04	C_{14}-NH_2	DEG	-0.388	0.092	1.79
L-05	Vinyl-BA	Benzaldehyde	0.450	0.153	7.87	S-05	Vinyl-BA	DEG	-0.330	0.221	13
L-06	Vinyl-BA	1,3-Dioxolane	0.428	1.175	45.28	S-06	CN-BA	Formamide	-0.171	0.151	1.89
Average			0.459	0.577	27.25	Average			-0.362	0.094	6.70
Standard deviation			0.018	0.371	22.61	Standard deviation			0.105	0.078	6.01
Tungstate											
Rank	Guest molecules	Medium	Predicted R_L / -	Measured R_L / -	Yield / %	Rank	Guest molecules	Medium	Predicted R_L / -	Measured R_L / -	Yield / %
L-01	Vinyl-BA	THF	0.473	N. A.	0	S-01	BPA	DEG	-0.460	0.046	26.73
L-02	H-BA	Benzaldehyde	0.469	0.044	6.43	S-02	API	DEG	-0.411	0.053	28.60
L-03	Vinyl-BA	Ethylbenzene	0.465	N. A.	0	S-03	C_6-NH_2	DEG	-0.394	0.199	6.51
L-04	CH_3-BA	Benzaldehyde	0.451	0.027	24.61	S-04	C_{14}-NH_2	DEG	-0.388	0.025	9.21
L-05	Vinyl-BA	Benzaldehyde	0.450	N. A.	0	S-05	Tp-EA	DEG	-0.337	0.234	44.15
L-06	Tp-EA	Benzaldehyde	0.442	0.222	25.83	S-06	CH_3-BA	DEG	-0.325	0.103	24.88
Average			0.458	0.098	9.48	Average			-0.386	0.110	23.35
Standard deviation			0.012	0.094	12.45	Standard deviation			0.050	0.087	13.84
Niobate											
Rank	Guest molecules	Medium	Predicted R_L / -	Measured R_L / -	Yield / %	Rank	Guest molecules	Medium	Predicted R_L / -	Measured R_L / -	Yield / %
L-01	Tp-EA	THF	0.461	N. A.	5.77	S-01	DAMN	Formamide	-0.567	0.025	28.71
L-02	CH_3-BA	Benzaldehyde	0.451	0.287	29.45	S-02	API	DEG	-0.476	0.204	7.07
L-03	Tp-EA	Benzaldehyde	0.442	0.180	46.4	S-03	Tp-EA	DEG	-0.411	0.054	7.04
L-04	CH_3-BA	1,3-Dioxolane	0.430	0.248	23.9	S-04	DAMN	Water	-0.353	0.045	24.37
L-05	C_6-NH_2	THF	0.419	0.402	71.04	S-05	CH_3-BA	DEG	-0.325	0.178	61.69
L-06	Tp-EA	1,3-Dioxolane	0.407	0.387	34.85	S-06	DEA	Formamide	-0.262	0.082	93.51
Average			0.435	0.301	41.13	Average			-0.399	0.098	37.07
Standard deviation			0.020	0.094	18.68	Standard deviation			0.110	0.075	34.13
Tantalate											
Rank	Guest molecules	Medium	Predicted R_L / -	Measured R_L / -	Yield / %	Rank	Guest molecules	Medium	Predicted R_L / -	Measured R_L / -	Yield / %
L-01	Vinyl-BA	THF	0.473	0.756	51.24	S-01	DAMN	Formamide	-0.567	0.185	11.91
L-02	CH_3-BA	Benzaldehyde	0.451	0.462	35.69	S-02	Tp-EA	DEG	-0.411	0.075	4.51
L-03	Vinyl-BA	Benzaldehyde	0.450	0.513	36.13	S-03	C_6-NH_2	DEG	-0.394	0.090	11.29
L-04	CH_3-BA	1,3-Dioxolane	0.430	1.091	48.16	S-04	C_{14}-NH_2	DEG	-0.388	0.328	10.32
L-05	C_6-NH_2	THF	0.419	N. A.	11.19	S-05	F-BA	DEG	-0.382	0.211	23.24
L-06	F-BA	Benzaldehyde	0.389	0.375	24.63	S-06	DAMN	Water	-0.353	0.181	4.11
Average			0.435	0.639	34.51	Average			-0.416	0.178	10.90
Standard deviation			0.029	0.289	14.91	Standard deviation			0.076	0.092	6.94
$Co(OH)_2$											
Rank	Guest molecules	Medium	Predicted R_L / -	Measured R_L / -	Yield / %	Rank	Guest molecules	Medium	Predicted R_L / -	Measured R_L / -	Yield / %
L-01	CH_3-PA	THF	0.426	0.471	41.81	S-01	TDS	DEG	-0.631	0.428	15.4
L-02	CH_3-PA	Benzaldehyde	0.410	0.135	6.05	S-02	AQS	Formamide	-0.523	N. A.	1.97
L-03	CH_3-PA	1,3-Dioxolane	0.368	0.228	66.95	S-03	BuO-PA	DEG	-0.441	0.044	4.89
L-04	C_6-COOH	THF	0.363	0.175	81.85	S-04	C_6-COOH	DEG	-0.441	0.067	16.83
L-05	BuO-PA	THF	0.357	0.210	62.72	S-05	CH_3-PA	DEG	-0.372	0.031	29.24
L-06	BuO-PA	Benzaldehyde	0.346	0.626	91.19	S-06	AQS	Water	-0.327	0.072	77.19
Average			0.378	0.308	58.43	Average			-0.456	0.129	24.25
Standard deviation			0.032	0.196	30.77	Standard deviation			0.109	0.168	27.68

Note: The abbreviations of the guest and medium molecules were described in Fig. S2. The exfoliated nanosheets were not observed for the combinations noted N. A.

The top 10 or 6 combinations for the large (L-01–10 or L-01–06) and small (S-01–10 or S-01–06) nanosheets are prepared using the size prediction model (eq. 1). The preparation procedure was described in the note in Fig. S2. Fig. 3 was prepared by the predicted and measured R_L values in Table S2.

Precursor layered composites based on titanate

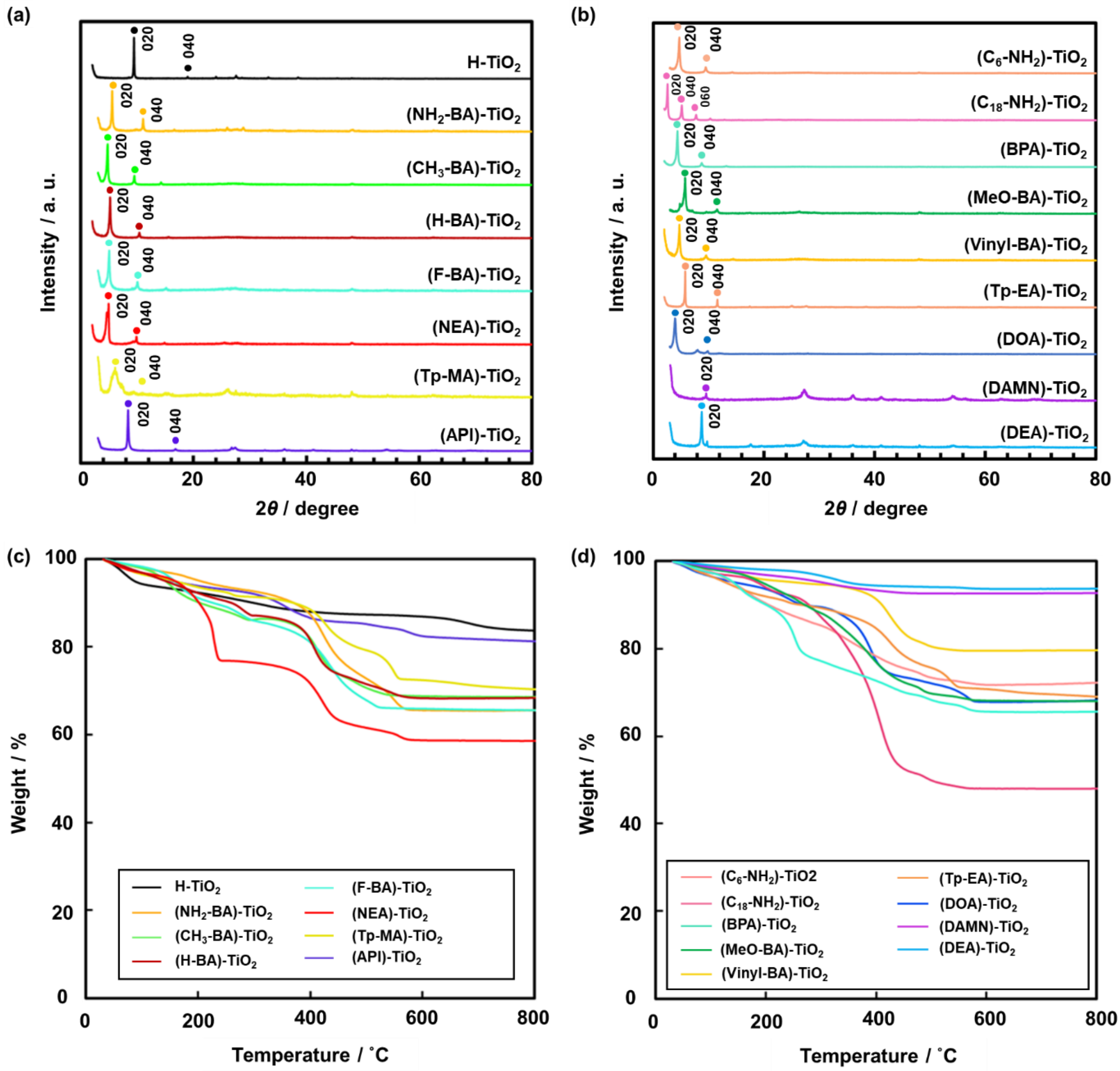

Fig. S3. XRD patterns (a,b) and TG-DTA curves (c,d) of the precursor layered composites based on titanate. The abbreviations are referred to Fig. S2.

The interlayer distance (d_0) and compositions (x, y) depended on the types of the intercalated guests. These data were summarized in Table S3. In the present work, the chemical formulae of the layered titanate were defined as (guest)$_x$H$_{0.7-x}$Ti$_{1.825}\square_{0.175}$O$_4\cdot y$H$_2$O (□: vacancy), according to previous reports.[12,44,R1]

Precursor layered composites based on manganate

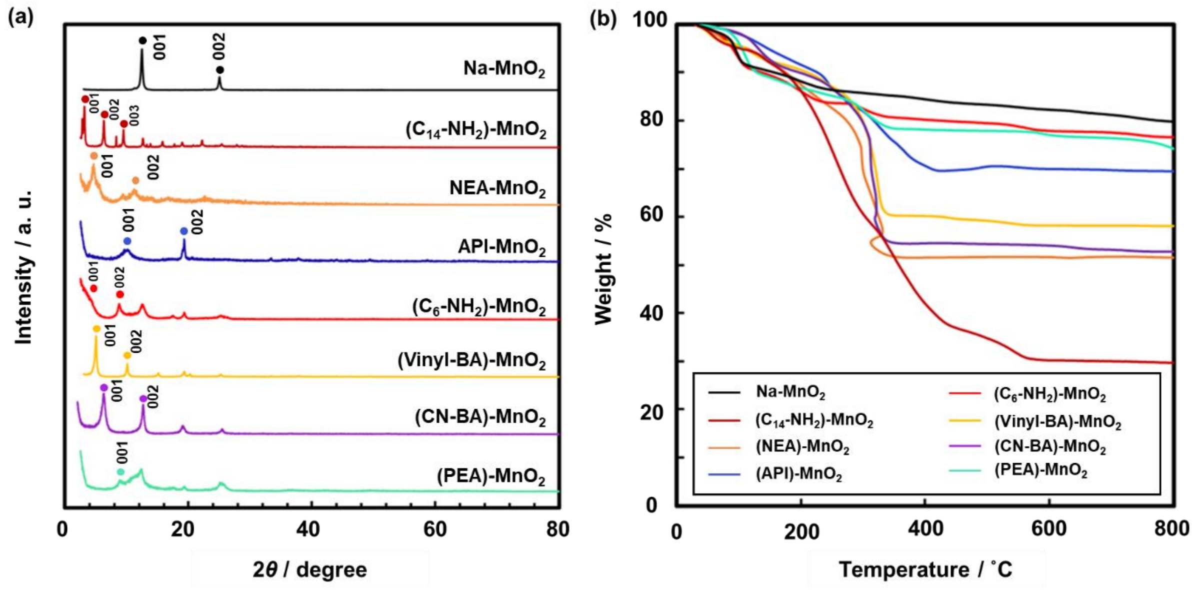

Fig. S4. XRD patterns (a) and TG-DTA curves (b) of the precursor layered composites based on manganate. The abbreviations are referred to Fig. S2.

The interlayer distance (d_0) and compositions (x, y) depended on the types of the intercalated guests. These data were summarized in Table S3. In the present work, the chemical formulae of the layered manganate were defined as (guest)$_x$Mn$_{2-x}$O$_2$·yH$_2$O, according to previous reports.[44,R2]

Precursor layered composites based on tungstate

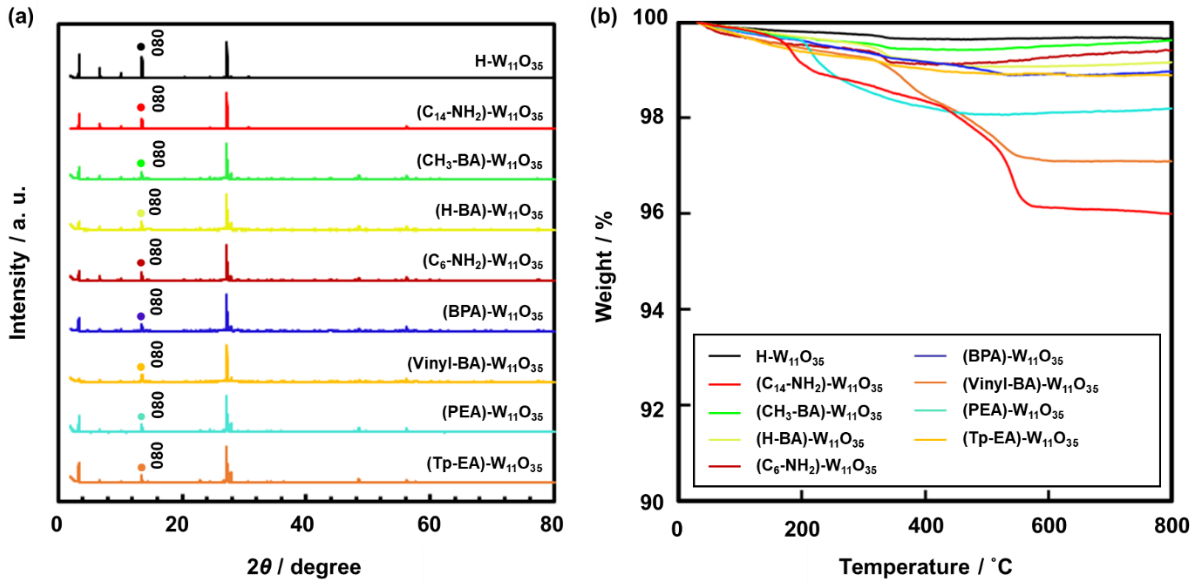

Fig. S5. XRD patterns (a) and TG-DTA curves (b) of the precursor layered composites based on tungstate. The abbreviations are referred to Fig. S2.

The compositions (x, y) depended on the types of the intercalated guests. These data were summarized in Table S3. In the present work, the chemical formulae of the layered manganate were defined as $(\text{guest})_x H_{1-x} Cs_3 W_{11} O_{35} \cdot y H_2O$, according to previous reports.[29,44,R3] The shift of (080) (d_0) peak was not observed for the layered tungstate (Fig. S5a). However, the TG curves showed the weight loss depending on the intercalated organic guests in the range of 200–500 °C (Fig. S5b). The results imply that the organic guests are intercalated in the interlayer space with lower tilted angle near the horizonal orientation to the layers. In our previous report, [29] the similar intercalation behavior was observed on layered tungstate.

Precursor layered composites based on niobate

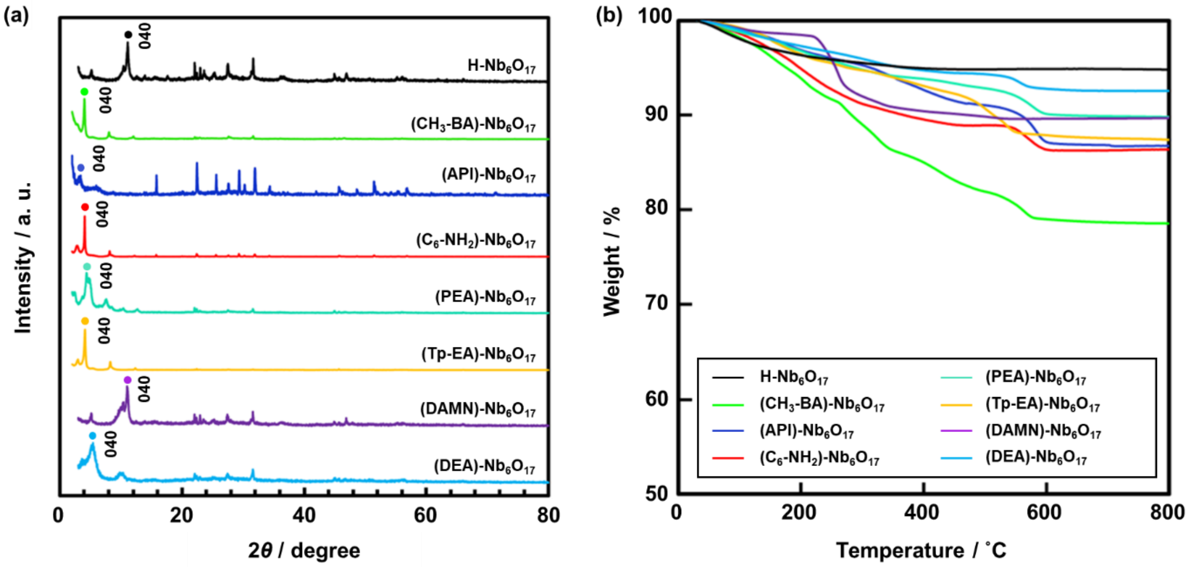

Fig. S6. XRD patterns (a) and TG-DTA curves (b) of the precursor layered composites based on niobate. The abbreviations are referred to Fig. S2.

The interlayer distance (d_0) and compositions (x, y) depended on the types of the intercalated guests. These data were summarized in Table S3. In the present work, the chemical formulae of the layered niobate were defined as (guest)$_x$Nb$_{6-x}$O$_{17}$·yH$_2$O (□: vacancy), according to previous reports.[59,60]

Precursor layered composites based on tantalate

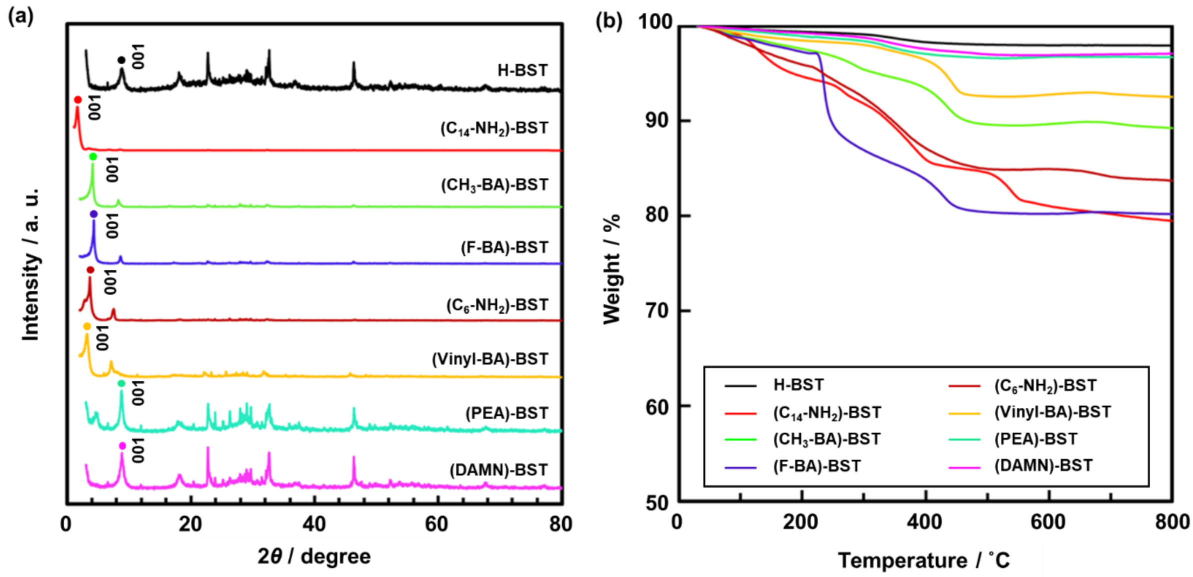

Fig. S7. XRD patterns (a) and TG-DTA curves (b) of the precursor layered composites based on tantalate. The abbreviations are referred to Fig. S2.

The interlayer distance (d_0) and compositions (x, y) depended on the types of the intercalated guests. These data were summarized in Table S3. In the present work, the chemical formulae of the layered tantalate were defined as $H_{1.8-x}(guest)_x Bi_{0.2}Sr_{0.8}Ta_2O_7 \cdot yH_2O$ (□: vacancy), according to previous reports.[61,62]

Precursor layered composites based on $Co(OH)_2$

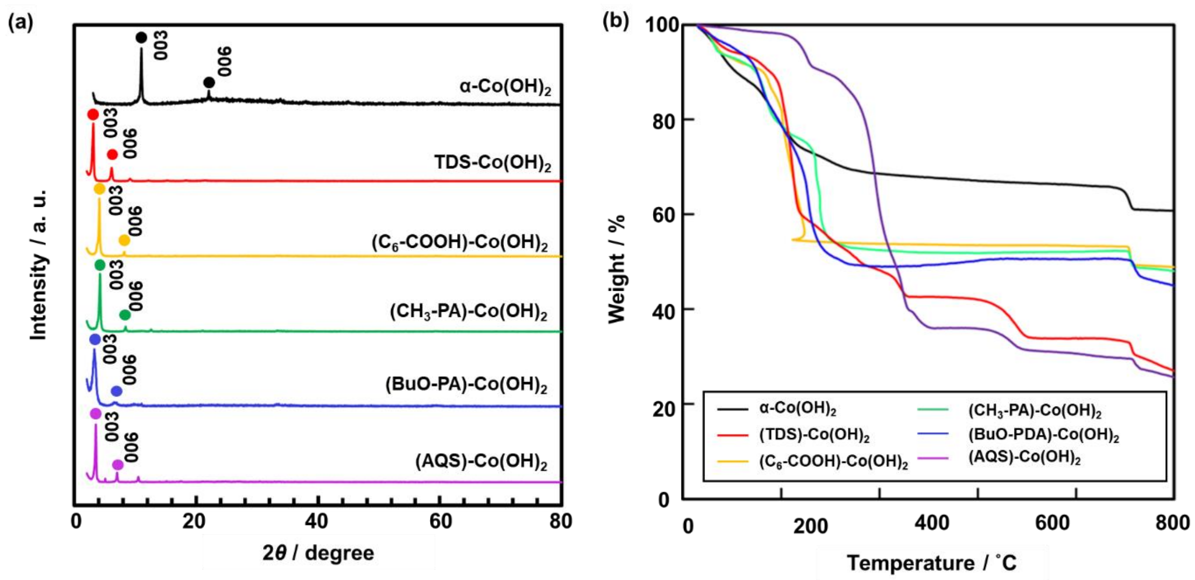

Fig. S8. XRD patterns (a) and TG-DTA curves (b) of the precursor layered composites based on $Co(OH)_2$. The abbreviations are referred to Fig. S2.

The interlayer distance (d_0) and compositions (x, y) depended on the types of the intercalated guests. These data were summarized in Table S3. In the present work, the chemical formulae of the layered $Co(OH)_2$ were defined as $(\text{guest})_x Co(OH)_2 \cdot y H_2O$ (□: vacancy), according to previous reports.[42,44,R4]

Structures and compositions of the precursor layered composites

Table S3. Interlayer distances and compositions of the precursor layered composites.

Titanate Guest	Interlayer distance d_{020} / nm	Composition x / –	Water content y / –
Pristine	0.939	–	0.789
C_{14}-NH_2	2.975	0.487	1.115
NH_2-BA	1.602	0.566	0.632
CH_3-BA	1.872	0.396	1.216
H-BA	1.696	0.546	0.987
F-BA	1.773	0.494	1.158
NEA	1.806	0.487	1.418
Tp-MA	1.456	0.462	0.782
API	1.061	0.201	0.644
C_6-NH_2	1.853	0.437	1.165
C_{18}-NH_2	3.426	0.580	1.094
BPA	4.373	0.450	1.293
MeO-BA	1.534	0.457	0.809
Vinyl-BA	1.852	0.253	0.453
Tp-EA	1.525	0.442	1.011
DOA	2.203	0.268	0.674
DAMN	0.915	0.0692	0.286
DEA	1.011	0.0747	0.174
Manganate Guest	Interlayer distance d_{001} / nm	Composition x / –	Water content y / –
Pristine	0.707	–	0.629
C_{14}-NH_2	2.805	0.640	1.835
NEA	1.902	0.346	1.077
API	0.891	0.239	0.553
C_6-NH_2	1.000	0.143	0.855
Vinyl-BA	1.755	0.367	0.725
CN-BA	1.420	0.344	0.839
PEA	0.988	0.169	0.856
Tungstate Guest	Interlayer distance d_{080} / nm	Composition x / –	Water content y / –
Pristine	0.653	–	0.582
C_{14}-NH_2	0.653	0.455	0.723
Me-BA	0.653	0.139	1.480
H-BA	0.653	0.219	0.582
C_6-NH_2	0.653	0.584	0.535
BPA	0.653	0.336	0.651
Vinyl-BA	0.653	0.667	0.919
PEA	0.653	0.446	0.660
Tp-EA	0.653	0.328	1.034
Niobate Guest	Interlayer distance d_{040} / nm	Composition x / –	Water content y / –
Pristine	0.793	–	1.83
Me-BA	2.202	1.503	3.79
API	2.839	0.876	1.75
C_6-NH_2	2.169	1.016	2.90
PEA	2.046	0.652	1.75
Tp-EA	2.158	0.806	1.98
DAMN	0.797	0.868	0.826
DEA	1.623	0.498	1.42

Table S3. Continued.

Tantalate Guest	Interlayer distance d_{001} / nm	Composition x / –	Water content y / –
Pristine	1.028	–	1.319
C_{14}-NH_2	5.399	0.557	2.199
CH_3-BA	2.138	0.530	0.890
F-BA	2.056	1.076	1.123
C_6-NH_2	2.411	0.966	1.609
Vinyl-BA	2.749	0.351	0.544
PEA	1.935	0.154	0.361
DAMN	1.000	0.151	0.247
$Co(OH)_2$ Guest	Interlayer distance d_{003} / nm	Composition x / –	Water content y / –
Pristine	0.804	–	0.970
TDS	2.869	0.365	1.925
C_6-COOH	2.169	0.308	1.618
CH_3-PA	2.116	0.364	1.040
BuO-PA	2.715	0.228	2.138
AQS	2.539	0.787	0.344

The interlayer distances (d_0) and compositions of the guests (x) and water content (y) were estimated from the XRD patterns and TG curves in Figs. S3–S8. The calculation methods of the compositions (x, y) were described in the Experimental Section and our previous works.[44]

DLS charts of the large- and small-size titanate nanosheets

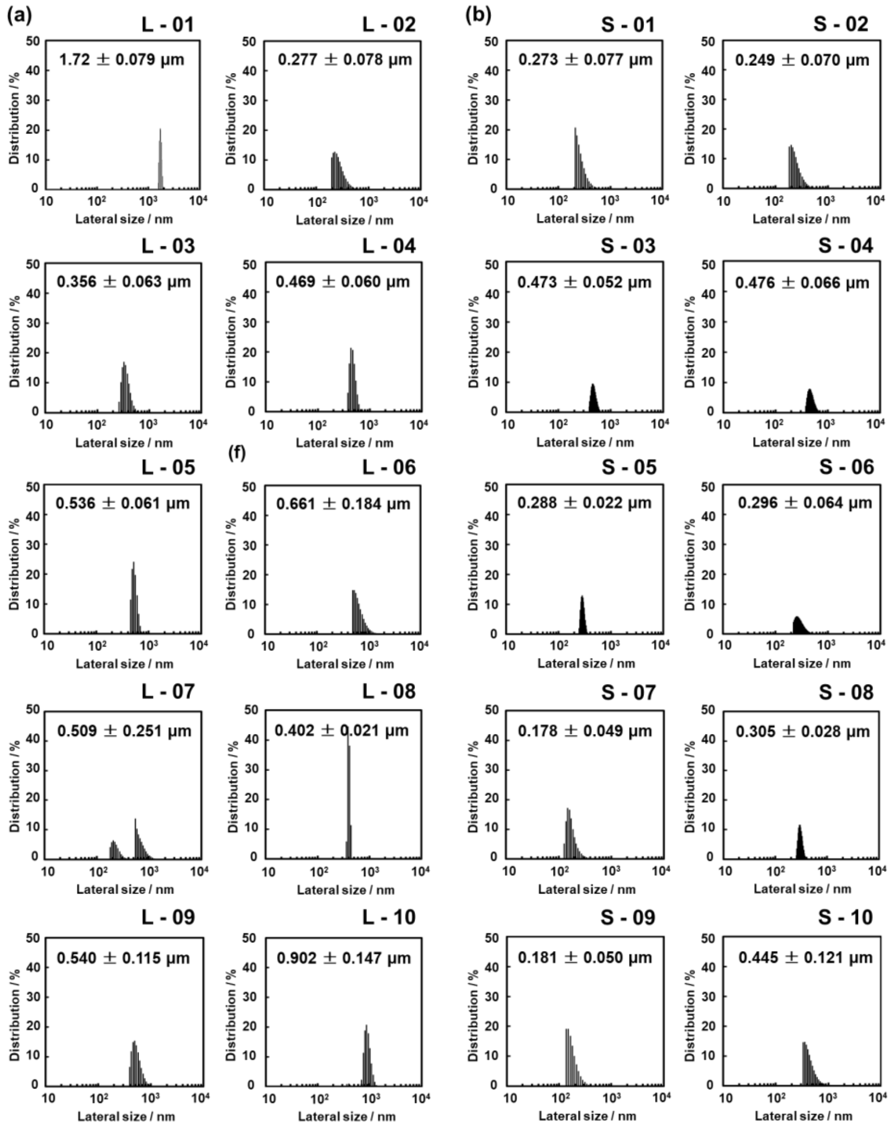

Fig. S9. DLS charts of the dispersion liquid containing titanate nanosheets for the predicted 10 guest-medium combinations providing large- (a, L-01–10) and small- (b, S-01–10) size nanosheets (Table S2).

DLS charts of the large- and small-size manganate nanosheets

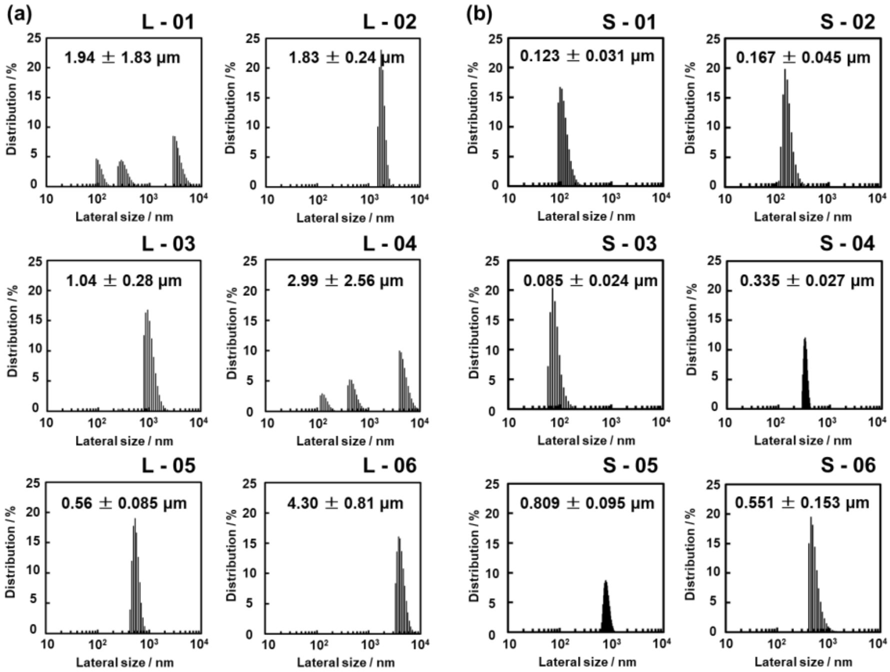

Fig. S10. DLS charts of the dispersion liquid containing manganate nanosheets for the predicted 6 guest-medium combinations providing large- (a, L-01–06) and small- (b, S-01–06) size nanosheets (Table S2).

DLS charts of the large- and small-size tungstate nanosheets

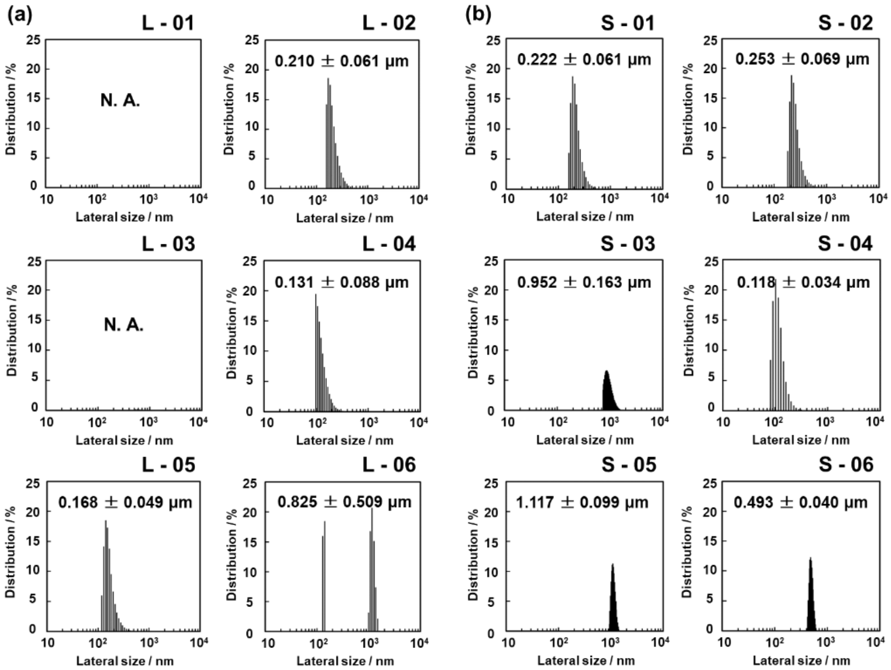

Fig. S11. DLS charts of the dispersion liquid containing tungstate nanosheets for the predicted 6 guest-medium combinations providing large- (a, L-01–06) and small- (b, S-01–06) size nanosheets (Table S2).

DLS charts of the large- and small-size niobate nanosheets

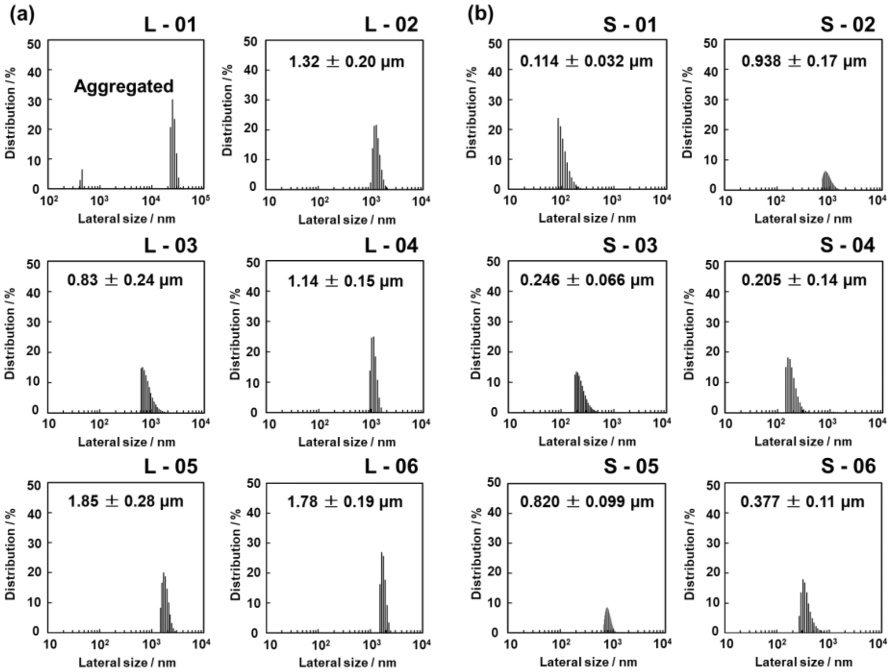

Fig. S12. DLS charts of the dispersion liquid containing niobate nanosheets for the predicted 6 guest-medium combinations providing large- (a, L-01–06) and small- (b, S-01–06) size nanosheets (Table S2).

DLS charts of the large- and small-size tantalate nanosheets

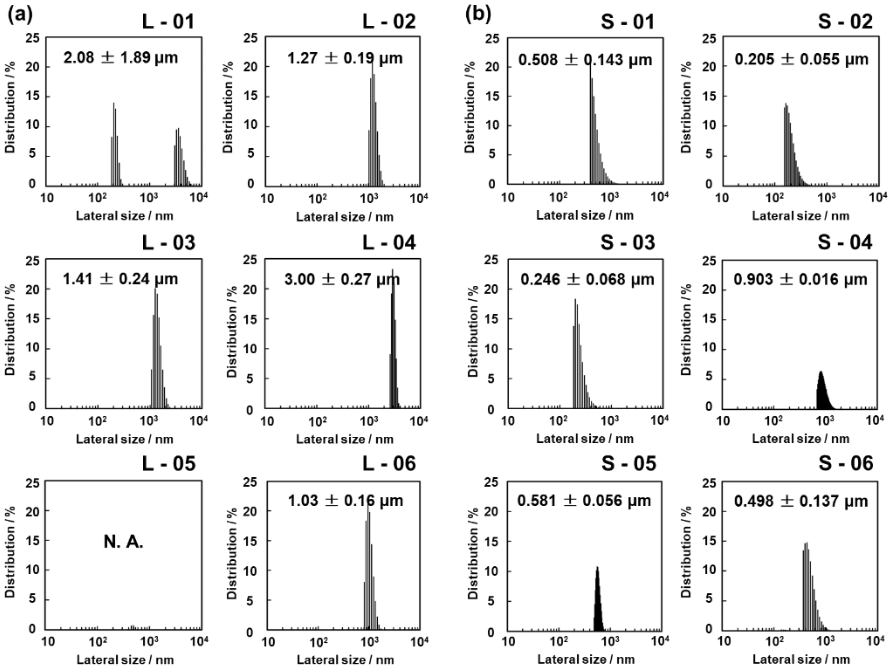

Fig. S13. DLS charts of the dispersion liquid containing tantalate nanosheets for the predicted 6 guest-medium combinations providing large- (a, L-01–06) and small- (b, S-01–06) size nanosheets (Table S2).

DLS charts of the large- and small-size $Co(OH)_2$ nanosheets

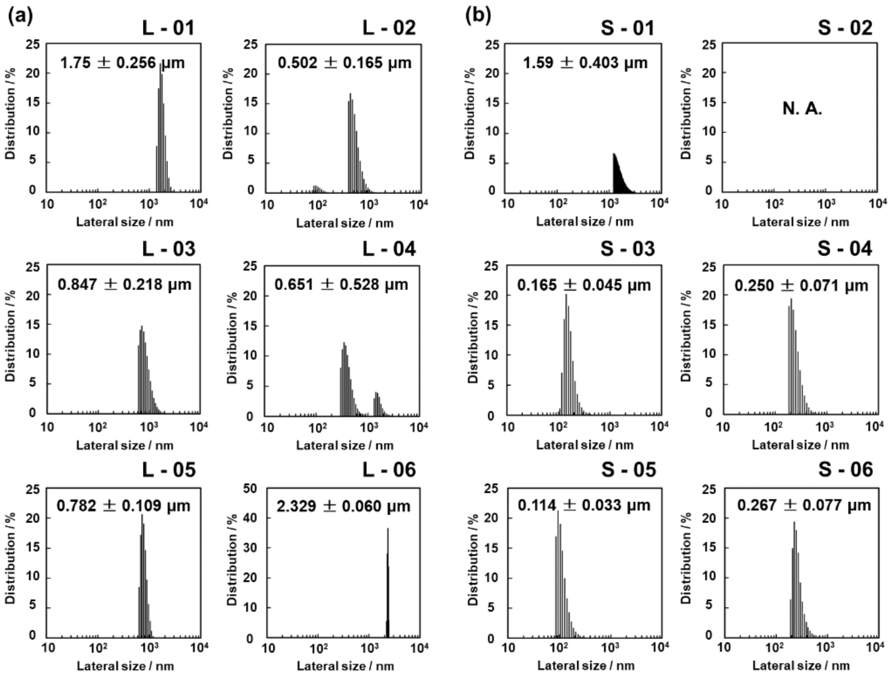

Fig. S14. DLS charts of the dispersion liquid containing $Co(OH)_2$ nanosheets for the predicted 6 guest-medium combinations providing large- (a, L-01–06) and small- (b, S-01–06) size nanosheets (Table S2).

TEM images of the resultant nanosheets

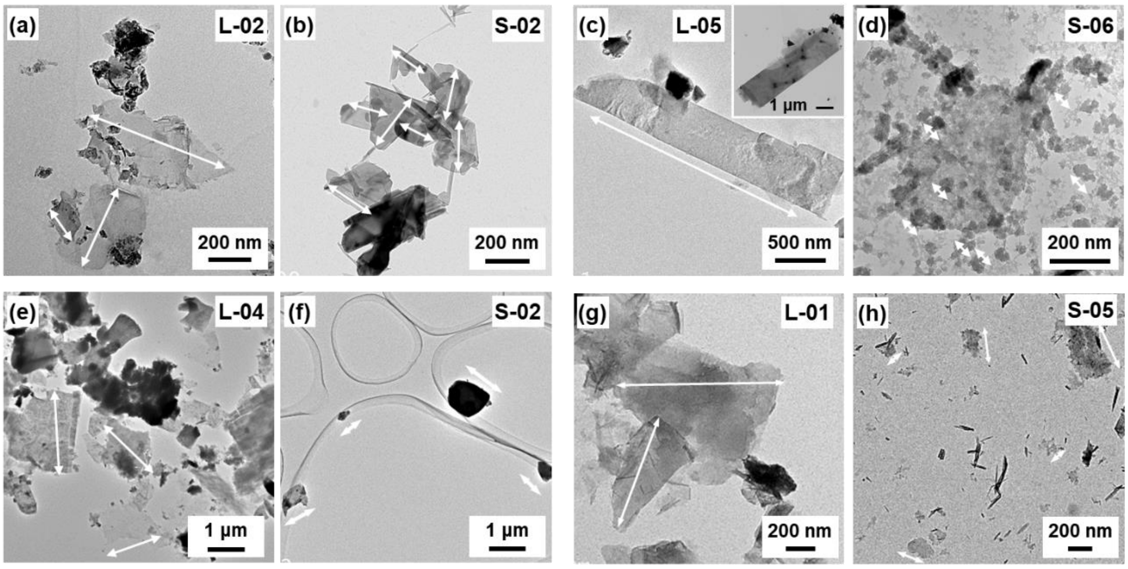

Fig. S15. TEM images of the large (a,c,e,g) and small (b,d,f,h) manganate (a,b), niobate (c,d), tantalate (e,f), and $Co(OH)_2$ (g,h) nanosheets. (a,b) Nanosheets exfoliated from the layered composites based on titanate with intercalation of VBA (L-02) and API (S-02) in THF and DEG, respectively. (c,d) Nanosheets exfoliated from the layered composites based on manganate with intercalation of C_6-NH_2 (L-05) and DEA (S-06) in THF and formamide, respectively. (e,f) The layered composites based on tantalate with intercalation of CH_3-BA (L-04) and Tp-EA (S-02) exfoliated in 1,3-dioxolane and DEG, respectively. (g,h) Nanosheets exfoliated from the layered composites based on titanate with intercalation of CH_3-PA (L-01, S-05) in THF and DEG, respectively.

Our group defined the monolayers and few-layers as the nanosheets. Therefore, the resultant dispersion liquid containing the nanosheets were obtained by the filtration of the unexfoliated bulky objects. Since the dispersion liquid was not purified by the centrifugation, the tiny fractured 0D nanoparticles were observed on the microscopy images. In fact, such 0D particles were not observed in our previous works about the similar surface-modified monolayers when the dispersion liquid was purified by centrifugation.[40]